Limit Cycle Analysis of Nonlinear Multivariable Feedback Control Systems

by TAIN-SOU TSAY *and* KUANG-WEI HAN

Institute of Electronics, Department of Electrical Engineering, National Chiao-Tung University, Taiwan, Republic of China

ABSTRACT: *A practical method is presented for the analysis of limit cycles in multivariable feedback control systems having separable nonlinear elements. The limit cycles are found by use of a criterion generated by the stability-equation method. Numerical examples are given and compared to other methods in the current literature.*

I. Introduction

In this paper, a practical method is presented which can be used to analyse the limit cycles of nonlinear multivariable feedback control systems having separable nonlinear elements. The general configuration of the considered nonlinear systems is shown in Fig. 1, where $N(\mathbf{a})$ and $G(S)$ represent the nonlinear and linear parts of the system, respectively. The method is based upon the stability-equation method which has been widely used for single-input–single-output nonlinear feedback control systems (**1–5**). The basic approach is to consider the equivalent gains of the nonlinearities as parameters to be analysed in the parameter-plane (**1–5**), and then the describing-function method is used to evaluate the amplitudes of the limit cycles at the inputs of nonlinearities.

In current literature, for multivariable systems the Nyquist, inverse Nyquist, and numerical optimization methods are usually used to predict the existence of limit cycles. These methods are based upon the graphical or numerical solutions of the linearized harmonic balance equations (**6–14**). It has been shown that, for multivariable systems, over arbitrary ranges of amplitudes (A_i), frequency (ω) and phases (θ_i), an infinite number of possible solutions may exist (**14**). Gray has proposed a sequential computational procedure to seek the solutions for only specified ranges of discrete values of A_i, ω and θ_i (**12–14**); these specified ranges are determined by use of the Nyquist or inverse Nyquist plots. Although the aforementioned methods are powerful, large computational efforts are usually required.

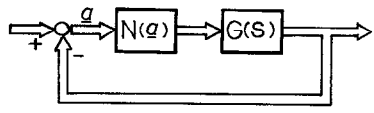

FIG. 1. A general block diagram of nonlinear multivariable feedback control systems.

It will be shown in this paper that the proposed method can give a single set of solutions (A_i, ω) mathematically, and the derivations of these solutions are very simple.

II. The Basic Approach

Consider the system shown in Fig. 1. The linearized harmonic balance equations (**12–14**) governing the existence of limit cycles can be expressed as:

$$[G(S)N(\mathbf{a})+I]\mathbf{a} = 0, \tag{1}$$

where $N(\mathbf{a})$ is a matrix of describing functions of the nonlinear elements, and $\mathbf{a}$ is a column vector of sinusoidal inputs to these nonlinear elements, such that

$$a_i = A_i \exp[j(\omega t+\theta_i)] \qquad (i = 1, 2, \ldots, n), \tag{2}$$

where A_i are the amplitudes of a_i; θ_i are the phase angles about a reference input; and n is the number of nonlinearities.

From (1) and (2), one can see that the number of parameters to be found is larger than that of the linearized harmonic balance equations. Therefore, an infinite number of possible solutions (**14**) exist which can satisfy (1).

For illustration, assume that a 2×2 nonlinear multivariable system with two single valued nonlinearities in the diagonal terms is considered; the block diagram is shown in Fig. 2. The harmonic balance equations (**6–14**) of loop 1 and loop 2 are

$$A_1 e^{j\theta_1} N_1(a_1) g_{11}(j\omega) + A_2 e^{j\theta_2} N_2(a_2) g_{12}(j\omega) = -A_1 e^{j\theta_1} \tag{3}$$

and

$$A_1 e^{j\theta_1} N_1(a_1) g_{21}(j\omega) + A_2 e^{j\theta_2} N_2(a_2) g_{22}(j\omega) = -A_2 e^{j\theta_2} \tag{4}$$

respectively, where $g_{ij}(S)$ are the (i, j) elements of $G(S)$; $N_1(a_1)$ and $N_2(a_2)$ are the describing functions [or equivalent gains (**15, 16**)] of the nonlinearities N_1 and N_2, respectively.

Consider the input of N_1 as the reference input. Then one has $\theta_1 = 0$, and (3) gives:

$$e^{j\theta_2} = -\frac{A_1[1+N_1(a_1)g_{11}(j\omega)]}{A_2 N_2(a_2) g_{12}(j\omega)}. \tag{5}$$

Similarly, (4) gives

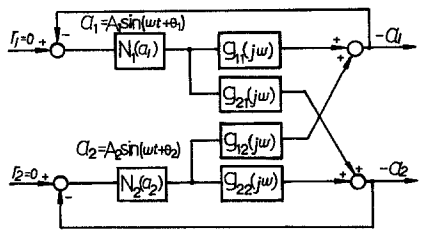

FIG. 2. Block diagram of a 2×2 nonlinear multivariable feedback control system.

$$e^{j\theta_2} = -\frac{N_1(a_1)g_{21}(j\omega)}{A_2[1+N_2(a_2)g_{22}(j\omega)]}. \tag{6}$$

Equating (5) and (6), one has

$$F(j\omega) = 1+N_1(a_1)g_{11}(j\omega)+N_2(a_2)g_{22}(j\omega) + N_1(a_1)N_2(a_2)[g_{11}(j\omega)g_{22}(j\omega)-g_{12}(j\omega)g_{21}(j\omega)] = 0 \tag{7}$$

which is the characteristic equation of the considered system. Note that $N_1(a_1)$ and $N_2(a_2)$ are considered as variable parameters.

Equation (7) can be decomposed into two stability equations (**1–5**); i.e.

$$F_e(\omega) = B_1(\omega) + N_1(a_1)C_1(\omega) + N_2(a_2)D_1(\omega) + N_1(a_1)N_2(a_2)E_1(\omega) = 0 \tag{8}$$

and

$$F_o(\omega) = B_2(\omega)+N_1(a_1)C_2(\omega)+N_2(a_2)D_2(\omega)+N_1(a_1)N_2(a_2)E_2(\omega) = 0. \tag{9}$$

Equation (8) gives

$$N_2(a_2) = -\frac{B_1(\omega)+N_1(a_1)C_1(\omega)}{D_1(\omega)+N_1(a_1)E_1(\omega)}. \tag{10}$$

Similarly, (9) gives

$$N_2(a_2) = -\frac{B_2(\omega)+N_1(a_1)C_2(\omega)}{D_2(\omega)+N_1(a_1)E_2(\omega)}. \tag{11}$$

Equating (10) and (11), one has

$$[C_2(\omega)E_1(\omega)-C_1(\omega)E_2(\omega)]N_1(a_1)^2+[C_2(\omega)D_1(\omega)+B_2(\omega)E_1(\omega) - C_1(\omega)D_2(\omega)-B_1(\omega)E_2(\omega)]N_1(a_1)+[B_2(\omega)D_1(\omega)-B_1(\omega)D_2(\omega)] = 0. \tag{12}$$

For specified values of frequency (ω), the values of $N_1(a_1)$ can be found by solving (12); the corresponding values of $N_2(a_2)$ can be found from (10), (11). For a number of suitable values of ω, the real solutions of $N_1(a_1)$ and $N_2(a_2)$ can be plotted in a $N_1(a_1)$ vs $N_2(a_2)$ plane. The typical result for a latter example is shown in Fig. 3.

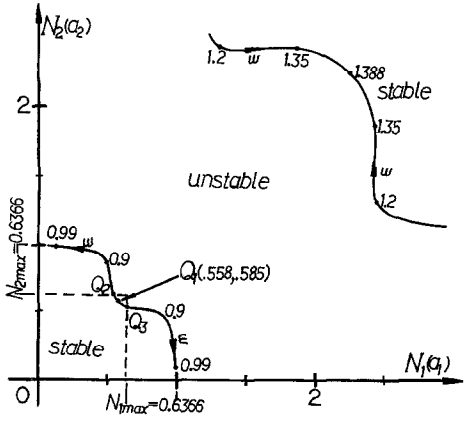

FIG. 3. Root-loci of the stability-equations for Example 1 with $K = 2$.

By use of Fig. 3, the conditions of having a limit cycle are explained as follows:

(i) Every point on the curves, as shown in Fig. 3, represents a set of $N_1(a_1)$, $N_2(a_2)$ and ω, which can satisfy the condition of having a limit cycle; i.e. the roots ω_{ei} and ω_{oj} of the even and odd stability equations $F_e(\omega)$ and $F_o(\omega)$, respectively, are all real and alternative in sequence except that one root pair is equal to each other (i.e. $\omega_{ei} = \omega_{oj} = \omega$) (**2–5**). But for nonlinear multivariable systems, an infinite number of solutions can satisfy this condition (**14**). This is quite different from the single-input–single-output system.

(ii) If the root-loci as shown in Fig. 3 separate the stable and unstable regions, then a limit cycle may exist. The reason is that the system will become stable or unstable when the amplitudes A_i increase or decrease. In other words, if the system becomes stable (unstable) when the amplitudes A_i increase (decrease), a stable limit cycle may exist at the stability boundary (**2–5**).

(iii) A limit cycle may exist only if the values of $N_1(a_1)$ and $N_2(a_2)$ are less than the maximal gains ($N_{1\max}$ and $N_{2\max}$) of the nonlinearities N_1 and N_2; e.g. in Fig. 3, the useful solution may exist only in the section between points Q_2 and Q_3.

(iv) A limit cycle may exist if the roots $N_1(a_1)$ and $N_2(a_2)$ satisfy (3) and (4). From (3) and (4), the possible solution can be found by equating the real and imaginary parts of (5) and (6), respectively; i.e.

$$|e^{j\theta_{25}} - e^{j\theta_{26}}| = 0 \tag{13}$$

where θ_{25} and θ_{26} represent the phase angles found by (5) and (6), respectively. Therefore, the values of A_1, A_2 and ω, for having a limit cycle, can be found from (8), (9) and (13).

If the considered nonlinear system satisfies all of the above four conditions, a limit cycle will exist. More explanations are given along with the numerical examples given in the next section.

III. Examples

Example 1

Assume that the system shown in Fig. 2 is a 2×2 system with transfer function matrix (**11**)

$$G(S) = \frac{K}{S(S+1)^2}\begin{bmatrix} 1 & 0.3 \\ -0.2S-0.2 & 1 \end{bmatrix} \tag{14}$$

where K represents the loop gains. The nonlinearities are two identical on–off relays with dead-zones having unit switching level and unit height.

From (7), the characteristic equation of the closed-loop system is

$$F(S) = S^6+4S^5+6S^4+4S^3+S^2+KN_1(a_1)(S^3+2S^2+S) + KN_2(a_2)(S^3+2S^2+S)+K^2N_1(a_1)N_2(a_2)(0.06S+1.06) = 0. \tag{15}$$

The stability equations are

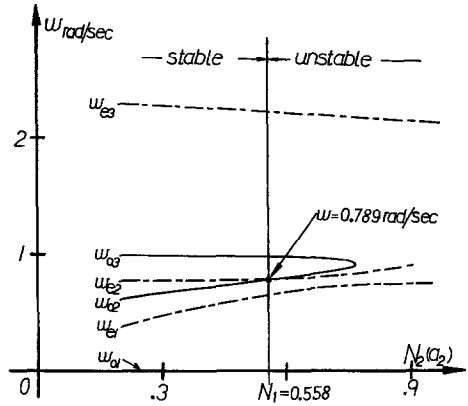

FIG. 4. Root-loci of ω_{ei} and ω_{oj} of the stability-equations with fixed $N_1(a_1)$ and varying $N_2(a_2)$.

$$F_e(\omega) = -\omega^6+6\omega^4-\omega^2+KN_1(a_1)(-2\omega^2)+KN_2(a_2)(-2\omega^2) + K^2N_1(a_1)N_2(a_2)(1.06) = 0 \quad (16)$$

and

$$F_o(\omega) = 4\omega^5-4\omega^3+KN_1(a_1)(-\omega^3+\omega)+KN_2(a_2)(-\omega^3+\omega) + K^2N_1(a_1)N_2(a_2)(0.06\omega) = 0. \quad (17)$$

For $K = 2$, and for a number of frequencies ω, the simultaneous solutions $[N_1(a_1)$ and $N_2(a_2)]$ of (16) and (17) are calculated and represented by two root-loci, as shown in Fig. 3, where the stability of each region is also shown. At every point on the root-loci, the roots ω_{ei} and ω_{oj} of the stability-equations $F_e(\omega)$ and $F_o(\omega)$ are all real and alternative in sequence except that one root pair is equal to each other (i.e. $\omega_{ei} = \omega_{oj} = \omega$).

In Fig. 3, it can be seen that the section between points Q_2 and Q_3 can satisfy conditions (i) to (iii). Solving (13) in this section, one has a limit cycle at point Q_1 (0.558, 0.585) with oscillating frequency $\omega = 0.789$ rad s^{-1}, and amplitudes $A_1 = 1.964$ and $A_2 = 1.818$. This fact is supported by checking the roots ω_{ei} and ω_{oj} of the stability-equations in the neighborhood of Q_1 (**5**). Figure 4 shows that the loci of ω_{ei} and ω_{oj} for $N_1(a_1)$ is fixed at 0.558 and $N_2(a_2)$ is varying. From Fig. 3, one can see that if the value of $N_2(a_2)$ is less (larger) than 0.585, the roots ω_{ei} and ω_{oj} are (not) alternative in sequence and the corresponding system is stable (unstable) (**2–5**). Therefore, a stable limit cycle will exist at the stability-boundary where $N_2(a_2) = 0.585$. Similar results can be obtained when $N_2(a_2)$ is fixed at 0.585 and $N_1(a_1)$ is varying. By computer simulation, Fig. 5 shows the limit cycle of the system for $K = 2$.

In current literature, the purpose of analysis is to find the minimum value of K for just having a limit cycle. In this paper, for various values of K the locus of Q_1 can be plotted easily, as shown in Fig. 6, where the minimum value of K is at point $Q_{1\min}$ where the values of $N_1(a_1)$ and $N_2(a_2)$ are just equal to the maximum values

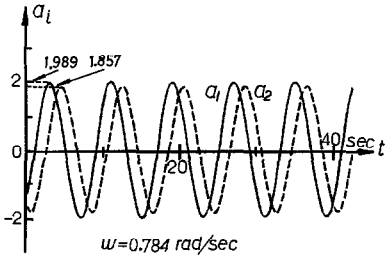

FIG. 5. The simulated limit-cycle of Example 1 for $K = 2$.

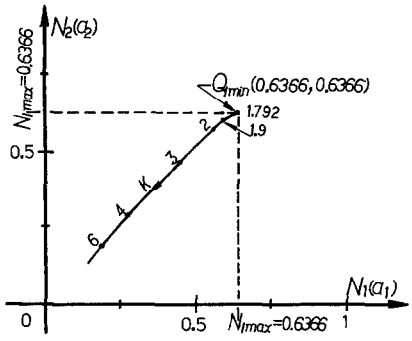

FIG. 6. Locus of Q_1 vs K.

TABLE I

The gains K *for just having a limit cycle in Example 1*

Methods	Gain K
Proposed method	1.79
Aizerman Conjecture	1.79
Hirsch plot	1.25
Mee plot	1.50
Digital simulation	1.787

of the describing functions. For the system considered, the minimum value of K is found at 1.7924. From Ref. (**11**), the results obtained by the use of other methods, are shown in Table I. Although all the results are approximately the same, the proposed method is relatively simple in computation.

Example 2

Consider a nonlinear system with transfer function matrix (**16**)

$$G(S) = \frac{K}{\Delta(S)} \begin{bmatrix} 16S^2+23S+9 & 4S^2-S-3 \\ 4S^2-S-3 & 16S^2+23S+9 \end{bmatrix} \tag{18}$$

where $\Delta(S) = (2S^3+4.2S^2+2.8S+0.6)/\exp(-0.1S)$. The two nonlinearities N_1

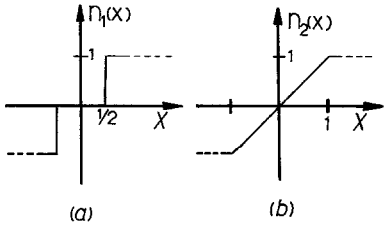

FIG. 7. Nonlinearities of Example 2.

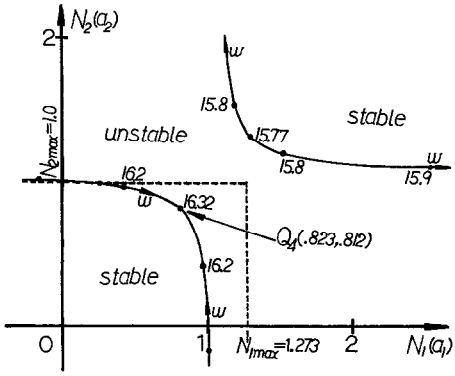

FIG. 8. Root-loci of stability equations for Example 2 with $K = 2$.

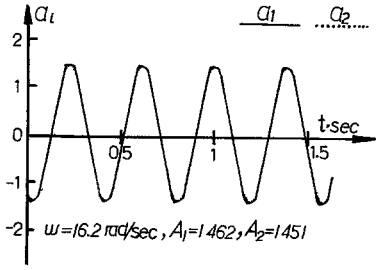

FIG. 9. The simulated limit-cycle of Example 2 for $K = 2$.

and N_2 are different, as shown in Fig. 7. Similar to the procedure stated in Example 1, the root-loci of the stability-equations for $K = 2$ are plotted, as shown in Fig. 8, where point Q_4 (0.823, 0.812) with oscillating frequency $\omega = 16.32$ rad s^{-1}, and amplitudes $A_1 = 1.454$ and $A_2 = 1.427$ can satisfy all the conditions of having a limit cycle. Figure 9 shows the simulated limit cycle of the system, in which a_1 is almost identical to a_2. It can be seen that the simulated results are quite close to those obtained by calculation.

Table II shows the values of K for just having a limit cycle predicted by various methods (**8**, **16**).

Example 3

Consider a coupled-core reactor (**17**, **18**) with system configuration, as shown in Fig. 10, where

TABLE II

The gains K for just having a limit cycle in Example 2

Methods	Gain K
Proposed method	1.28
Ramani and Atherton	1.29
Kouvaritakis and Cameron	1.06
Digital simulation	1.16

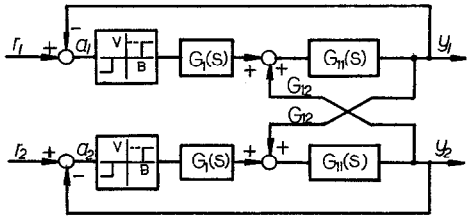

FIG. 10. Block diagram of a control system for a coupled-core reactor.

$$G_{11}(S) = \frac{(S+a)(S+\lambda)}{\left(S+\frac{2r}{\tau}\right)(S+\lambda)(S+a)+\frac{\beta}{\tau}S(S+a)+\frac{\alpha h n_0}{\tau}(S+\lambda)} \tag{19}$$

$$G_{12}(S) = \frac{2r}{\tau} \tag{20}$$

and

$$G_1(S) = \frac{n_0}{\tau S(1+T_m S)}. \tag{21}$$

Assume that the parameters of the system are $\beta = 0.0049$, $\lambda = 0.44$, $\tau = 0.0001$ s, $h = 10°\text{F/(MW s)}$, $a = 10\ \text{s}^{-1}$, $\alpha = 0.001°\text{F}^{-1}$, $n_0 = 30$ MW, $r = 0.018$, $T_m = 0.07$ s, and the parameters of the nonlinearities, shown in Fig. 10, are $B = 0.25$ MW and $V = M \times 10^{-3}\ \delta k/k \cdot \text{s}$ (**17**, **18**). For $M = 22$, by use of the same procedure stated in Example 1, the root-loci of the stability-equations are shown in Fig. 11, where point Q_5 (0.052, 0.052) with oscillating frequency $\omega = 60.93$ rad s^{-1}, and amplitudes $A_1 = 0.446$ MW and $A_2 = 0.446$ MW satisfies all the conditions of having a limit cycle. The simulated result is shown in Fig. 12. (Note that a_1 is identical to a_2 because the considered system is symmetrical.) This is quite close to that obtained by calculation.

From all the above examples, it can be seen that the proposed method provides a simple way for predicting the existence of limit cycles of nonlinear multivariable feedback control systems, and that in each system a unique solution can be obtained using simple calculations.

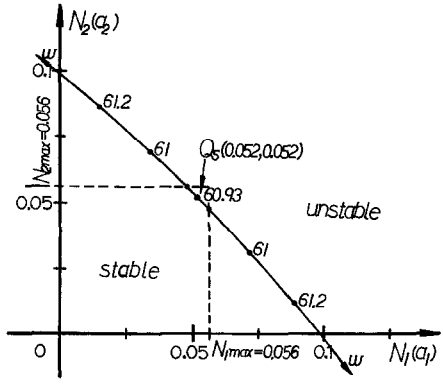

FIG. 11. Root-loci of stability equations for Example 3.

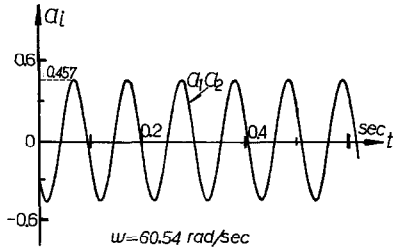

FIG. 12. The simulated limit-cycle of Example 3 for $M = 22$ and $B = 0.25$ MW.

IV. Conclusions

In this paper, a method for limit cycle analysis in nonlinear multivariable feedback control systems has been presented, and found to be simpler than other methods given in the current literature. It has been shown that the proposed method can be easily applied to very complicated systems.

References

(1) K. W. Kan and G. J. Thaler, "High Order System Analysis and Design using the Root Locus Method", *J. Franklin Inst.*, Vol. 281, No. 2, pp. 99–113, Feb. 1966.

(2) K. W. Han, "Nonlinear Control System: Some Practical Method", Academic Culture Company, 1977.

(3) Y. L. Chen and K. W. Han, "Stability Analysis of a Nonlinear Reactor Control System", *IEEE Trans. Nucl. Sci.*, Vol. NS-17, No. 2, pp. 18–25, April 1970.

(4) C. H. Ai and K. W. Han, "Stability Analysis of Nuclear Reactor Control System with Multiple Transport-lags and Asymmetrical Nonlinearity", *IEEE Trans. Nucl. Sci.*, Vol. NS-22, No. 5, Oct. 1975.

(5) T. S. Tsay and K. W. Han, "Analysis of a Nonlinear Sampled-data Proportional Navigation System having Adjustable parameters", *J. Franklin Inst.*, Vol. 321, No. 4, pp. 203–218, April 1986.

(6) D. P. Atherton, "Nonlinear Control Engineering", Van Nostrand–Reinhold, London, 1975.

(7) A. I. Mees, "Describing Functions, Circle Criteria and Multiloop Feedback Systems", *PROC. IEE*, Vol. 120, No. 1, pp. 126–130, 1973.
(8) N. Ramani and D. P. Atherton, "Frequency Response Method for Nonlinear Multivariable Systems", Canadian Conference on Automatic Control, University of New Brunswick, Fredericton, 1973.
(9) N. Ramani and D. P. Atherton, "A Describing Function Method for the Approximate Stability of Nonlinear Multivariable Systems", University of New Brunswick, Electrical Engineering Department, Report SDC-1, 1975.
(10) S. Shankar and D. P. Atherton, "Graphical Stability Analysis of Non-linear Multivariable Control Systems", *Int. J. Control*, Vol. 25, pp. 375–388, 1977.
(11) A. K. El Shakkany and D. P. Atherton, "Computer graphics method for Nonlinear Multivariable Systems", *IFAC* Computer-Aided Design of Control Systems, pp. 157–161, 1979.
(12) J. O. Gray and P. M. Taylor, "Frequency Responses Method in the Design of Multivariable Nonlinear Feedback Systems", 4th IFAC, Multivariable Technological Systems, pp. 225–232, 1977.
(13) J. O. Gray and P. M. Taylor, "Computer Aided Design of Multivariable Nonlinear Control Systems using Frequency Domain Techniques", *Automatica*, Vol. 15, pp. 281–297, 1979.
(14) J. O. Gray and N. B. Nakhla, "Prediction of Limit Cycle in Multivariable Nonlinear Systems", *PROC. IEE*, Vol. 128, Pt.D, pp. 283–241, Sept. 1981.
(15) R. G. Cameron and M. Tabatabai, "Prediction of the Existence of Limit Cycles using Walsh Function: some Further Results", *Int. J. System Sci.*, Vol. 14, pp. 1043–1064, 1983.
(16) B. Kouvaritakis and R. G. Cameron, "The Use of Walsh Functions in Multivariable Limit Cycle Prediction", *Automatica*, Vol. 19, pp. 513–522, 1983.
(17) G. V. S. Raju and R. S. Stone, "Control System in Spatially Large Cores", *IEEE Trans. Nucl. Sci.*, Vol. NS-17, pp. 534–540, Feb. 1970.
(18) N. Tsouri, J. Rootenberg and L. J. Lidofsky, "Stability Analysis of a Reactor Control System by the Tsypkin Locus Method", *IEEE Trans. Nucl. Sci.*, Vol. NS-20, No. 1, pp. 649–660, Feb. 1973.